Available online at www.sciencedirect.com
ScienceDirect
Journal of Computational Physics 225 (2007) 1199–1210
JOURNAL OF COMPUTATIONAL PHYSICS
www.elsevier.com/locate/jcp

Short Note

Cancellation problem of preconditioning method at low Mach numbers

Sang-Hyeon Lee *

Department of Aerospace Engineering, University of Ulsan, Mugeo-Dong, Nam-Gu, Ulsan 680-749, Republic of Korea

Received 18 December 2006; received in revised form 13 March 2007; accepted 2 April 2007
Available online 5 April 2007

Abstract

The effects of cancellation errors on the convergence characteristics of preconditioned Navier–Stokes equations at low Mach numbers are analyzed. Laminar viscous flows around a circular cylinder are calculated at different Mach numbers. It is shown that the cancellation error in the energy equation grows faster than those in the other equations, as the Mach number decreases. It is also shown that the cancellation problem of the energy equation is due to the off-diagonal element that is related to a pressure change in the preconditioner.

Keywords: Cancellation errors; Preconditioning; Flows at low Mach numbers; Convergence

1. Introduction

Preconditioning methods have received growing attention due to their various applications in CFD fields. The difficulty in solving the compressible flow at a low Mach number is associated with the large disparity in the magnitudes of eigenvalues, which is called eigenvalue stiffness [1]. The preconditioning method pre-multiplies the time derivative by a suitable preconditioner that scales the eigenvalues to the same order of magnitude. A number of preconditioning approaches have been suggested to solve the stiffness problem [2–9]. Choi and Merkle [5] suggested a preconditioner that introduced well-conditioned eigenvalues and has been extended for use in many CFD applications [6,7,10–13].

Lee [16] reported that preconditioned Euler equations have serious convergence problems at low Mach numbers and that there is a Mach number limit where converged solutions could not be obtained. This is attributed to cancellation errors that occur due to accumulation effects of round-off errors. Round-off errors are mainly determined by the precision of floating-point variables and thus are inevitable. However, as shown by Sesterhenn et al. [17], cancellation errors can be avoided to a certain extent by a proper manipulation. Lee [16] reported that the convergence characteristics are strongly related to the behavior of the preconditioner,

* Tel.: +82 52 259 2825; fax: +82 52 259 1681.
E-mail address: lsh@mail.ulsan.ac.kr

0021-9991/$ - see front matter © 2007 Elsevier Inc. All rights reserved.
doi:10.1016/j.jcp.2007.04.001

while Sesterhenn et al. [17] paid their attention to the effects of the cancellation errors on the spatial discretization. However, they did not address the relationship between cancellation errors and convergence characteristics. In the present study, the relationship between cancellation errors and convergence characteristics will be thoroughly analyzed.

2. Cancellation errors

2.1. Governing equations

The governing equations considered in the present study are the two-dimensional preconditioned Navier–Stokes equations

$$\Gamma\frac{\partial Q}{\partial t}+\frac{\partial E}{\partial x}+\frac{\partial F}{\partial y}=\frac{\partial E_v}{\partial x}+\frac{\partial F_v}{\partial y}, \tag{2.1.1a}$$

$$Q=\begin{bmatrix}p\\u\\v\\T\end{bmatrix},\quad E=\begin{bmatrix}\rho u\\ \rho u^2+p\\ \rho uv\\ \rho h_o u\end{bmatrix},\quad F=\begin{bmatrix}\rho v\\ \rho uv\\ \rho v^2+p\\ \rho h_o v\end{bmatrix},\quad E_v=\begin{bmatrix}0\\ \tau_{xx}\\ \tau_{xy}\\ u_j\tau_{xj}-q_x\end{bmatrix},\quad F_v=\begin{bmatrix}0\\ \tau_{yx}\\ \tau_{yy}\\ u_j\tau_{yj}-q_y\end{bmatrix}, \tag{2.1.1b}$$

$$\Gamma=\begin{bmatrix}\frac{1}{\beta} & 0 & 0 & 0\\ \frac{u}{\beta} & \rho & 0 & 0\\ \frac{v}{\beta} & 0 & \rho & 0\\ \frac{h_0}{\beta}-1 & \rho u & \rho v & \rho c_p\end{bmatrix}, \tag{2.1.1c}$$

$$\beta=c^2M_r^2,\quad M_r^2=\min[1,\max(M^2,0.25M_\infty^2)]. \tag{2.1.1d}$$

Density is determined by the thermodynamic state equation, $p=\rho RT$. The preconditioner, Γ, considered in the present study is Choi and Merkle's preconditioner. Multiplying the system of equations by the inverse of the preconditioner results in a different form of the system of equations as follows:

$$\frac{\partial Q}{\partial t}+\Gamma^{-1}\left(\frac{\partial E}{\partial x}+\frac{\partial F}{\partial y}\right)=\Gamma^{-1}\left(\frac{\partial E_v}{\partial x}+\frac{\partial F_v}{\partial y}\right), \tag{2.1.2a}$$

$$\Gamma^{-1}=\begin{bmatrix}\beta & 0 & 0 & 0\\ -\frac{u}{\rho} & \frac{1}{\rho} & 0 & 0\\ -\frac{v}{\rho} & 0 & \frac{1}{\rho} & 0\\ \frac{\beta-h_0+u^2+v^2}{\rho c_p} & -\frac{u}{\rho c_p} & -\frac{v}{\rho c_p} & \frac{1}{\rho c_p}\end{bmatrix}. \tag{2.1.2b}$$

The transformed system of Eqs. (2.1.2) is mathematically the same as the original system of Eqs. (2.1.1). However, these systems of equations are different from each other in numerical terms. This will be discussed in later section.

The governing equations are non-dimensionalized with the quantities at the infinite far field: p_∞ (static pressure), ρ_∞ (density), T_∞ (temperature), c_∞ (speed of sound), R_∞ (gas constant), γ_∞ (specific heats ratio), μ_∞ (viscosity), and L (characteristic length).

$$\begin{aligned}&\hat{p}=\frac{p}{\gamma_\infty p_\infty},\quad \hat{\rho}=\frac{\rho}{\rho_\infty},\quad \hat{T}=\frac{T}{\gamma_\infty T_\infty},\quad \hat{u}=\frac{u}{c_\infty},\quad \hat{v}=\frac{v}{c_\infty},\quad \hat{h}_o=\frac{h_o}{c_\infty^2},\\ &\hat{R}=\frac{R}{R_\infty},\quad \hat{c}_p=\frac{c_p}{R_\infty},\quad \hat{\mu}=\frac{\mu}{\mu_\infty},\quad \hat{x}=\frac{x}{L},\quad \hat{y}=\frac{y}{L},\quad \hat{t}=\frac{tc_\infty}{L}.\end{aligned} \tag{2.1.3}$$

As shown in the previous study [16], the non-dimensionalized governing equations are of the same form as the original equations. Hereafter, the hat notations will be dropped for convenience. The non-dimensionalized quantities have the following orders of magnitude:

$$u, v \sim \mathrm{O}(M), \quad p, \rho, T \sim \mathrm{O}(1), \quad h_o \sim \mathrm{O}(1), \quad R, c_p \sim \mathrm{O}(1), \quad \beta \sim \mathrm{O}(M^2). \tag{2.1.4}$$

2.2. Error analysis

The numerical operator that expresses round-off errors during arithmetic operations is defined as follows:

$$\langle a * b \rangle = (a * b)(1 + \varepsilon). \tag{2.2.1}$$

The operator "$*$" denotes one of the floating-point arithmetic operators. The error is estimated as $|\varepsilon| \leqslant 5 \times 10^{-d}$ when d decimals are available for representation of the mantissa. A machine provides various precisions of floating-point variable such as "single," "double" or "extended double" precisions. Thus, the magnitude of d is determined due to the machine itself and the precision provided by the machine.

The most common serious problems resulting from a round-off error occur in cases where many steps are involved with rounding occurring at each step, or when two quantities very close to each other are subtracted or when a number is divided by another number close to zero [18]. Let the "serious" round-off error be symbolized as "δ" to distinguish it from the "normal" round-off error "ε". Let the round-off error ε be a constant for simplicity.

In the present study, low Mach number flows will be considered, since the cancellation effects appear at low Mach numbers. Also, the explicit calculations are considered for simplicity. The explicit form of the discretized system of equations can be expressed as follows:

$$\Gamma \Delta Q = \mathrm{RES}, \tag{2.2.2a}$$

$$\mathrm{RES} = [R_P, R_u, R_v, R_T]^{\mathrm{T}} = -\Delta t \left[\frac{\Delta(E - E_v)}{\Delta x} - \frac{\Delta(F - F_v)}{\Delta y} \right]. \tag{2.2.2b}$$

Assume that the residual vector, RES, is a well discretized or an error-free one. The change of solution vector, ΔQ, can be expressed in the following form:

$$\Delta p = \langle \beta R_P \rangle = \beta R_P (1 + \varepsilon), \tag{2.2.3a}$$

$$\begin{aligned} \Delta u &= \left\langle \frac{1}{\rho} \left\langle R_u - \left\langle \left\langle \frac{u}{\beta} \right\rangle \Delta p \right\rangle \right\rangle \right\rangle = \frac{1}{\rho} \left[R_u - u \frac{\Delta p}{\beta} (1 + \delta_u)(1 + \varepsilon) \right] (1 + \varepsilon)^2 \\ &\approx \frac{R_u - u R_P}{\rho} - \frac{u}{\rho} \frac{\Delta p}{\beta} (\delta_u + \varepsilon), \end{aligned} \tag{2.2.3b}$$

$$\begin{aligned} \Delta T &= \left\langle \frac{1}{\rho c_p} \left\langle R_T - \left\langle \left\langle \frac{\langle h_0 - \beta \rangle}{\beta} \right\rangle \Delta p \right\rangle + \langle \langle \rho u \rangle \Delta u \rangle + \langle \langle \rho v \rangle \Delta v \rangle \right\rangle \right\rangle \\ &= \frac{1}{\rho c_p} \left\{ R_T - \left[\frac{(h_0 - \beta)\Delta p}{\beta} (1 + \delta_T) + (\rho u \Delta u + \rho v \Delta v) \right] (1 + \varepsilon)^2 \right\} (1 + \varepsilon)^2 \\ &\approx \frac{1}{\rho c_p} \left[R_T - \frac{(h_0 - \beta)\Delta p}{\beta} - \rho(u \Delta u + v \Delta v) \right] - \frac{1}{\rho c_p} \left[(h_0 - \beta) \Delta p \frac{(\delta_T + 2\varepsilon)}{\beta} + \rho(u \Delta u + v \Delta v) 2\varepsilon \right]. \end{aligned} \tag{2.2.3c}$$

The errors occurred during the operation of dividing by β are denoted as δ_u for momentum equation and δ_T for the energy equation, since β goes to zero as the Mach number approaches zero. The preconditioning parameter β is $c^2 M^2$ in subsonic flows. Ideal or error-free solutions are assumed and symbolized by Δp^*, Δu^*, ΔT^*. Then the errors occurring in the calculations are expressed in terms of the Mach numbers.

$$\Delta p - \Delta p^* = \Delta p - \beta R_P = \varepsilon, \tag{2.2.4a}$$

$$\Delta u - \Delta u^* = \Delta u - \frac{R_u - u R_P}{\rho} = -\frac{u \Delta p}{\rho c} \frac{\delta_u + \varepsilon}{\beta} \approx -\frac{\Delta p^*}{\rho c} \frac{\delta_u + \varepsilon}{M}, \tag{2.2.4b}$$

$$\Delta T - \Delta T^* = -\frac{h_0-\beta}{c^2\rho c_p}\Delta p\frac{\delta_T+2\varepsilon}{\beta} - \frac{u\Delta u + v\Delta v}{c_p}2\varepsilon \approx -\frac{h_0}{c^2\rho c_p}\Delta p^*\frac{\delta_T+2\varepsilon}{M^2}. \tag{2.2.4c}$$

The errors δ_u and δ_T grow as the Mach number decreases since dividing by β induces more serious errors as β approaches zero. However, δ_u would be smaller than δ_T by M, since $u \sim O(M)$ and $h_0 \sim O(1)$, as shown in Eq. (2.1.4). Thus the errors δ_u and δ_T can be expressed as follows:

$$\delta_u = \delta_u(M) = \varepsilon M^{-m}, \quad m > 0, \tag{2.2.5a}$$

$$\delta_T = \delta_T(M) = \varepsilon M^{-2m}, \quad m > 0. \tag{2.2.5b}$$

Then, considering the orders of the non-dimensionalized quantities, Eq. (2.2.4) can be reduced as follows:

$$\Delta u - \Delta u^* \sim -\Delta p^*\frac{\delta_u}{M} = -\Delta p^*\varepsilon M^{-(1+m)}, \tag{2.2.6a}$$

$$\Delta T - \Delta T^* \sim -\Delta p^*\frac{\delta_T}{M^2} = -\Delta p^*\varepsilon M^{-2(1+m)}. \tag{2.2.6b}$$

The pressure change is irrespective of the Mach number. While the velocity error grows by $M^{-(1+m)}$ and the temperature error grows by $M^{-2(1+m)}$, which implies that convergence problem in the energy equation is more serious than those in the other equations.

Now, consider the cancellation errors in the system of equations (2.1.2). The explicit form of the system of equations (2.1.2) can be expressed as follows:

$$\Delta Q = \Gamma^{-1}\mathrm{RES}. \tag{2.2.7}$$

The solution change ΔQ can be expressed in the following form:

$$\Delta p = \langle \beta R_P \rangle = \beta R_P(1+\varepsilon), \tag{2.2.8a}$$

$$\Delta u = \left\langle \frac{1}{\rho}\langle R_u - \langle uR_p\rangle\rangle \right\rangle = \frac{R_u - uR_P(1+\varepsilon)}{\rho}(1+\varepsilon)^2 \approx \Delta u^* - \frac{u}{\rho}\Delta p^*\frac{\varepsilon}{\beta}, \tag{2.2.8b}$$

$$\begin{aligned}\Delta T &= \left\langle \frac{1}{\rho c_p}\langle R_T - \langle\langle h_0-\beta-u^2-v^2\rangle R_p\rangle - \langle uR_u\rangle - \langle vR_v\rangle\rangle \right\rangle \\ &= \frac{R_T - [(h_0-\beta-u^2-v^2)R_P(1+\varepsilon) + uR_u + vR_v](1+\varepsilon)}{\rho c_p}(1+\varepsilon)^2 \\ &\approx \Delta T^* - \frac{h_0-\beta-u^2-v^2}{\rho c_p}\Delta p^*\frac{2\varepsilon}{\beta} - \frac{uR_u+vR_v}{\rho c_p}\varepsilon.\end{aligned} \tag{2.2.8c}$$

Then, the errors can be expressed in terms of the Mach number as follows:

$$\Delta u - \Delta u^* \sim -\Delta p^*\varepsilon M^{-1}, \tag{2.2.9a}$$

$$\Delta T - \Delta T^* \sim -\Delta p^*\varepsilon M^{-2}. \tag{2.2.9b}$$

The velocity error grows by M^{-1}, while the temperature error grows by M^{-2}, which implies that convergence problem in the energy equation is more serious than those in the other equations. Also, comparison between Eqs. (2.2.6) and (2.2.9) suggests that the transformation by multiplying the inverse of the preconditioner to the governing equations would alleviate cancellation problems.

Another important aspect related to the definition of the reference Mach number or preconditioning parameter is shown in Eqs. (2.2.6) and (2.2.9). As mentioned by Turkel [1], it is very difficult or impossible to obtain solutions of the Navier–Stokes equations with the definition for the Euler equations, $M_r^2 = \min(1, M^2)$. Eqs. (2.2.6) and (2.2.9) show that the cancellation errors go to infinity, if a local Mach number approaches zero. In viscous flows, there are many regions at a smaller Mach number than the free-stream Mach number, such as at a boundary layer and a wake. Thus, the cancellation errors in locally low speed regions are much larger than those in the surrounding regions, which would deteriorate the convergence characteristics. In order to avoid this problem, most of the previous studies [1–7,10–15] adopted a cut-off strategy as shown in Eq. (2.1.1d).

2.3. Effects of off-diagonal elements

As shown above, the cancellation error in the energy equation grows or is magnified through the off-diagonal element $h_0/\beta - 1$ in the preconditioner. This can be verified if an approximate preconditioner, by dropping the off-diagonal element in the energy equation, is introduced. The approximate preconditioner considered in the present study is

$$\Gamma = \begin{bmatrix} \frac{1}{\theta_P} & 0 & 0 & 0 \\ \frac{u}{\beta} & \rho & 0 & 0 \\ \frac{v}{\beta} & 0 & \rho & 0 \\ 0 & \rho u & \rho v & \frac{1}{\theta_T} \end{bmatrix}. \tag{2.3.1}$$

The term θ_T is introduced to compensate for the off-diagonal term $h_0/\beta - 1$ and the term θ_P is a modified β introduced to augment numerical stabilities. Let an approximate set of preconditioning parameters be introduced with an assumption that the solutions satisfy the isentropic relationship, $\Delta p/p = \gamma/(\gamma-1)\Delta T/T$. Then the parameters are as follows:

$$\frac{1}{\theta_P} = \frac{1}{\beta}\frac{\gamma}{\gamma-1}, \quad \frac{1}{\theta_T} = \rho c_p + \frac{T}{p}\left(\frac{h_o}{\beta} - 1\right). \tag{2.3.2}$$

This approach would lead to un-physical behavior of the solutions. However, it gives meaningful information about the effects of the cancellation errors. Then, the velocity change is the same as Eq. (2.2.8b). The pressure change and the temperature change become

$$\Delta p = \langle \theta_P R_P \rangle = \theta_P R_P (1+\varepsilon), \tag{2.3.3a}$$

$$\begin{aligned} \Delta T &= \langle \theta_T \langle R_T - \langle\langle \rho u \rangle \Delta u \rangle + \langle\langle \rho v \rangle \Delta v \rangle\rangle \rangle = \theta_T [R_T - (\rho u \Delta u + \rho v \Delta v)(1+\varepsilon)^2](1+\varepsilon)^2 \\ &\approx \theta_T [R_T - (\rho u \Delta u + \rho v \Delta v)] - \theta_T [\rho u \Delta u + \rho v \Delta v](2\varepsilon). \end{aligned} \tag{2.3.3b}$$

There is no serious cancellation error in the temperature field with the decrease of the Mach numbers since $\theta_T \sim O(M^2)$.

3. Numerical methods

3.1. Discretization

A finite volume method is used to discretize the preconditioned governing equations. In order to get the flux vector at the surface of a grid cell, the Roe type FDS (flux difference splitting) scheme suggested by Guillard and Viozat [19] is used. The van Albada limiter [20] is used to avoid numerical oscillations. The LU-SGS (lower upper symmetric Gauss Seidel) scheme [11,13] is used for time integration.

3.2. Grid system and boundary conditions

The calculations in the present study were conducted on an O-type grid system. The size of the computational domain is taken to be a sufficiently large domain, in order to minimize the boundary effects. The radius of the outer boundary is 60 times that of the cylinder diameter. The number of grid points is 10,800 (120×90). The grid points in the circumferential direction are evenly distributed and the grid points in the radial direction are clustered towards the cylinder wall up to where the aspect ratio of the nearest grid point from the wall is about unity.

The inflow and outflow boundaries were specified with the characteristic boundary conditions [1,21,22]. As suggested by Okong'o and Bellan [22], the density and velocity at the inflow boundary were fixed, and the pressure at the inflow boundary was updated according to the outgoing wave amplitude variations determined from interior points. The pressure at the outflow boundary was fixed, and the remaining wave amplitude variations were determined from the interior points. A no-slip boundary condition is applied at the solid walls. On

adiabatic walls, the temperature, density and pressure are determined to be the same as those at the nearest grid point.

3.3. Algorithms and precisions

In order to distinguish numerical methods, let symbols be introduced. Symbol "CM" denotes the method adopting the Choi and Merkle's preconditioner, symbol "CI" denotes the method adopting the system of governing equations (2.1.2) that is transformed by multiplying the inverse of the Choi and Merkle's preconditioner to the original system of governing equations (2.1.1), and symbol "AP" denotes the method adopting the approximate preconditioner (2.3.1).

The concept of relative treatments of all the variables and flux vectors, suggested by Lee [16] and Sesterhenn et al. [17], is adopted to reduce the cancellation errors.

$$\phi = \bar{\phi} + \phi', \quad \phi = u, v, h_o, p, T, \rho, \tag{3.3.1a}$$

$$E_k = \bar{E}_k + E'_k, \quad E_k = E, F. \tag{3.3.1b}$$

The part with an over-bar, $\bar{\phi}$, denotes a fixed one, while the part with a prime, ϕ', denotes a relative one.

The calculations were conducted using double precision ("double" in C language) floating-point variables that store 15 significant digits.

3.4. Estimation of convergence

The residual decays of velocity, pressure and temperature are plotted to represent the convergence characteristics. Lee [16] showed that it was necessary to renormalize the residuals in order to represent the convergence characteristics as follows:

$$\mathrm{RES}(p) = \frac{\sum_{i,j}|\Delta p|}{N_G M_\infty^2}, \quad \mathrm{RES}(u,v) = \frac{\sum_{i,j}\sum_{q=u,v}|\Delta q|}{N_G M_\infty}, \quad \mathrm{RES}(T) = \frac{\sum_{i,j}|\Delta T|}{N_G M_\infty^2}. \tag{3.4.1}$$

The term N_G denotes the number of grid points.

4. Calculation results

4.1. Verification of computational code

The laminar viscous flows around circular cylinders were calculated with various methods. Fig. 1 shows the flow fields around a circular cylinder at $Re = 20$ and $Re = 40$ that are obtained with method CM. The calculation results obtained with method CI are exactly same as those obtained with method CM. The flow pressure and temperature fields are well resolved and the recirculation flows are well captured. To verify the computation code used in the present study, the characteristics calculated in the present study are compared with those of the previous calculations [23–25]. The comparisons are shown in Table 1.

The maximum differences of the reattachment lengths, L_R, and the drag coefficients, C_D, among the methods are within 2%. Thus, the calculation methods used in the present study give reasonable results.

4.2. Effects of transformation of governing equations

Fig. 2 compares the convergence characteristics of methods CM and CI at $M = 10^{-2}$, 10^{-4} and 10^{-6}. The horizontal guidelines indicate the critical renormalized residuals required for enough convergence. There are slight differences between methods CM and CI in the convergences of the pressure field and the velocity field. However, method CM shows serious convergence problems in the energy equation. The renormalized temperature residual of method CM dramatically grows as the Mach number decreases, which means that the case at a lower Mach number needs a higher number of iterations to converge.

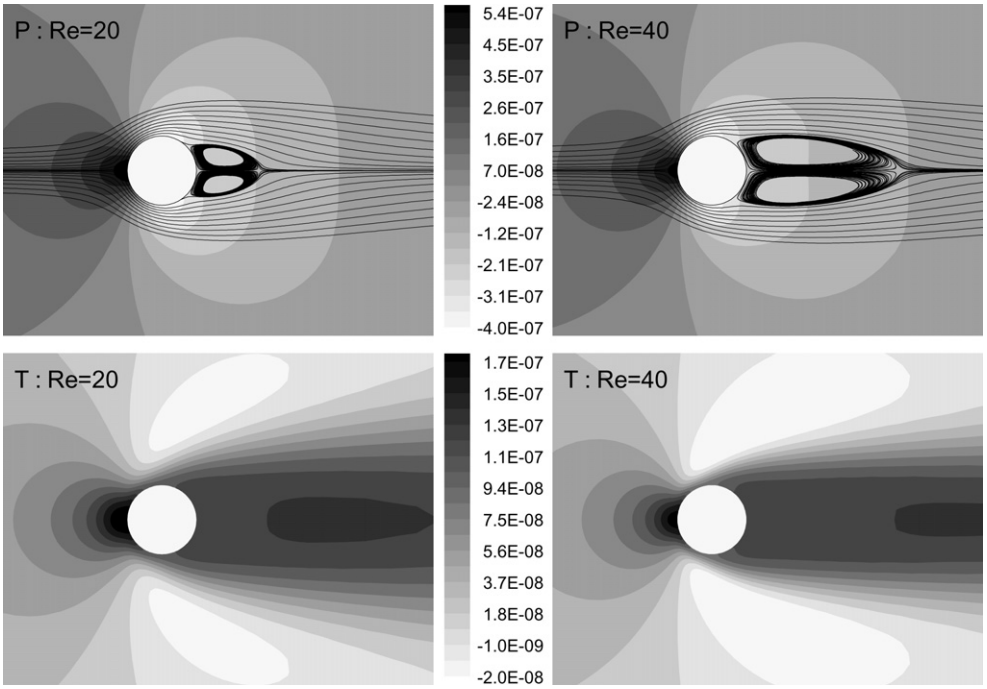

Fig. 1. Pressure fields, $(p - p_\infty)/p_\infty$, and temperature fields, $(T - T_\infty)/T_\infty$, at $Re = 20$ and $Re = 40$. The inflow Mach number is 10^{-3}.

Table 1
Characteristic numbers for flow past a circular cylinder

	$Re = 20$		$Re = 40$	
	L_R	C_D	L_R	C_D
Dennis and Chang [23]	0.94	2.05	2.35	1.52
Fornberg [24]	0.91	2.00	2.24	1.50
Linnick and Fasel [25]	0.93	2.06	2.28	1.54
Present (CM, CI)	0.93	2.04	2.24	1.54

Fig. 3 shows the changes of the temperature field according to the iteration. Method CI requires the same iterations to obtain converged temperature fields regardless of Mach numbers, while method CM requires more iterations as the Mach number decreases. This verifies that serious cancellation errors in method CM occur during the operation of dividing by β that goes to zero as the Mach number approaches zero, and that the transformation of the governing equations by multiplying the inverse of the preconditioner to the governing equations (2.1.1) alleviates serious cancellation problems.

4.3. Effects of off-diagonal elements

Fig. 4 compares the convergence characteristics of methods CI and AP at very low Mach numbers. For the calculations with method CI, the convergences of the continuity equation and the momentum equation at different Mach numbers are exactly same, respectively. However, when $M \leqslant 10^{-7}$, the energy equation does not converge over the guideline and the case at a lower Mach number shows a larger magnitude of the renormalized residual. However, for the calculations with method AP, the convergences of all the equations at different Mach numbers are exactly same, respectively. This suggests that these serious convergence problems, which are due to the cancellation errors, are strongly related to the off-diagonal element $h_0/\beta - 1$.

Fig. 5 shows the pressure fields and the temperature fields at very low Mach numbers. In the case where method CI is used, there are unphysical wiggle patterns in wake regions at $M = 10^{-7}$. Moreover, method

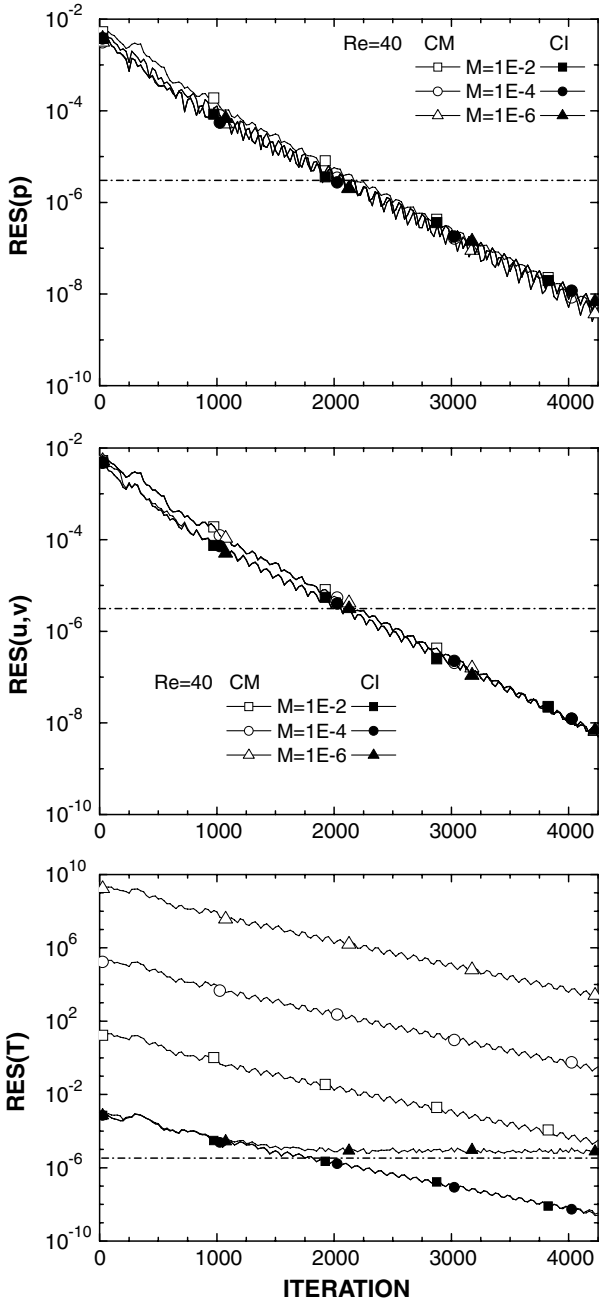

Fig. 2. Convergence histories of pressure, velocity and temperature at various Mach numbers.

CI cannot resolve any meaningful features of the temperature fields at $M = 10^{-8}$. Method AP gives a fully converged temperature field even at $M = 10^{-9}$. However, the temperature field calculated with method AP is exactly same as the pressure field and does not resolve temperature rises near the boundary layer and the wake region, which means that the approximate preconditioner equation (2.2.7) does not work well. Even though method AP does not provide a well-resolved temperature field, these results show clear evidence that the convergence problem in the energy equation is due to the cancellation errors that are magnified by the off-diagonal term $h_0/\beta - 1$.

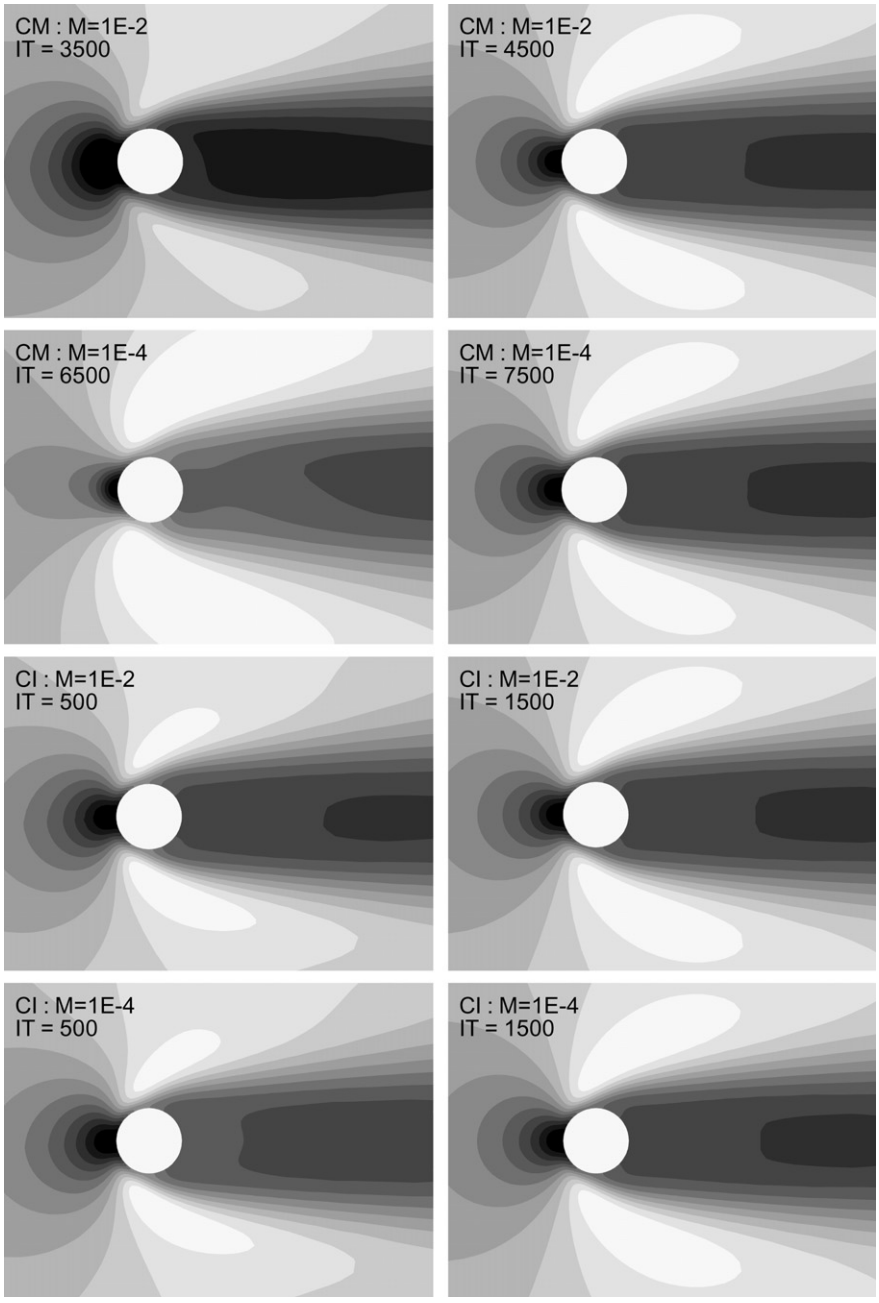

Fig. 3. Changes of temperature fields according to iterations at various Mach numbers. $Re = 40$.

5. Concluding remarks

An error analysis was conducted to analyze the influences of cancellation errors on the convergence characteristics of the Navier–Stokes equations and also numerical calculations were conducted to confirm the analysis.

When the Choi and Merkle's preconditioner is used, the renormalized temperature residual grows and thus the number of iterations required to obtain a fully converged temperature field increases as the Mach number

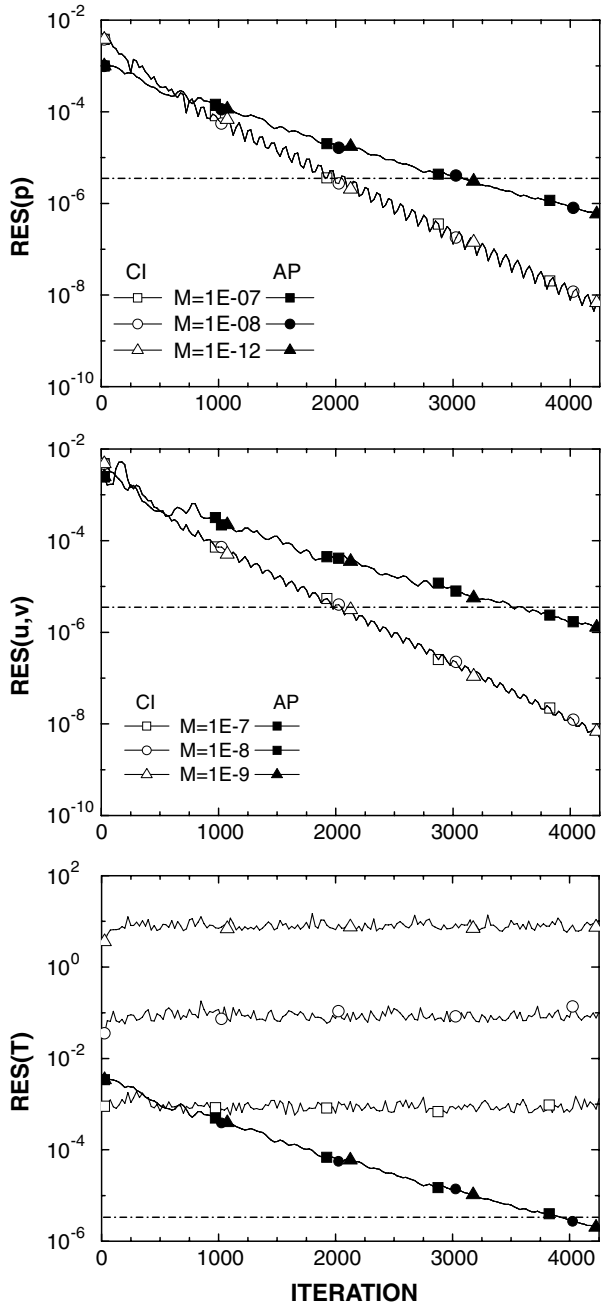

Fig. 4. Convergence histories of pressure, velocity and temperature at very low Mach numbers. $Re = 40$.

decreases. The transformation of the governing equations by multiplying the inverse of the preconditioner solves this kind of convergence problem.

It is difficult or impossible to obtain a fully converged temperature field at a Mach number below 10^{-6}, while the pressure field and velocity field can be obtained at a much lower Mach number. This is due to the fact that the cancellation errors in the energy equation grow faster than those in the continuity equation and the momentum equation, as the Mach number decreases. The calculation with an approximate

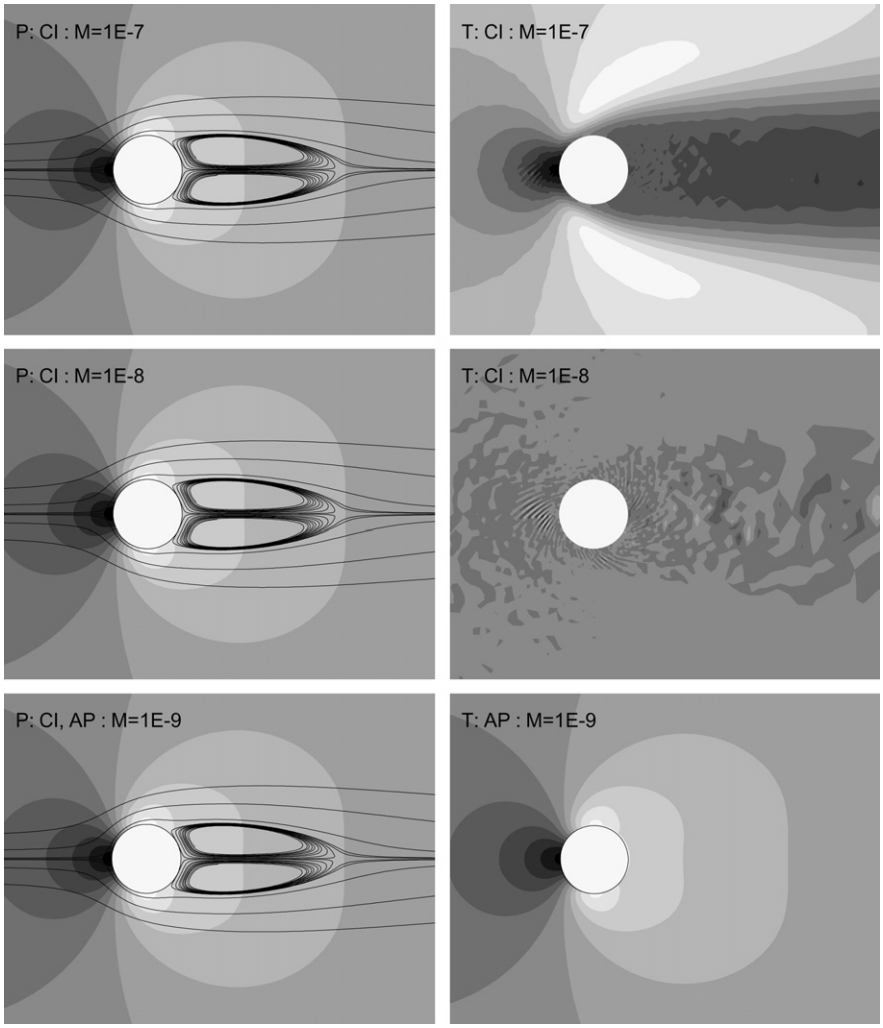

Fig. 5. Temperature field at various low Mach numbers. $Re = 40$.

preconditioner shows that the off-diagonal element related to the pressure change magnifies the round-off errors and prevents the energy equation from converging.

References

[1] E. Turkel, Annu. Rev. Fluid Mech. 31 (1999) 385.
[2] E. Turkel, J. Comput. Phys. 72 (1987) 277.
[3] E. Turkel, Appl. Numer. Math. 12 (1993) 257.
[4] B. van Leer, W-T. Lee, P. Roe, AIAA paper 91-1552-CP, 1991.
[5] Y.H. Choi, C.L. Merkle, J. Comput. Phys. 105 (1993) 207.
[6] J.M. Weiss, W.A. Smith, AIAA J. 33 (1995) 2050.
[7] C.J. Merkle, AIAA J. 36 (1998) 515.
[8] M. Sabanca, G. Brenner, N. Alemdaroglu, Int. J. Numer. Methods Fluids 34 (2000) 167.
[9] M. Sabanca, F. Durst, Phys. Fluids 15 (2003) 1821.
[10] J.S. Shuen, K.H. Chen, J. Comput. Phys. 106 (1993) 306.
[11] K.H. Chen, J.S. Shuen, AIAA paper 94-3047, 1994.
[12] K.H. Chen, J.S. Shuen, E. Mularz, AIAA paper 95-0800, 1995.
[13] L.D. Dailey, R.H. Pletcher, AIAA paper 95-1668, 1995.
[14] S. Hsieh, V. Yang, Int. J. CFD 8 (1997) 31.

[15] P. Buelow, D.A. Schwer, J. Feng, C.L. Merkle, AIAA paper 97-2101, 1997.
[16] S.-H. Lee, J. Comput. Phys. 208 (2005) 266.
[17] J. Sesterhenn, B. Muller, H. Thomann, J. Comput. Phys. 151 (1999) 597.
[18] S.D. Conte, C. de Boor, Elementary Numerical Analysis, McGraw-Hill, New York, 1988.
[19] S. Guillard, C. Viozat, Comput. Fluid 28 (1999) 63.
[20] P. Arminjon, A. St-Cyr, A. Madrane, Appl. Numer. Math. 40 (2002) 367.
[21] D.L. Darmofal, P. Moinier, M.B. Giles, J. Comput. Phys. 160 (2000) 369.
[22] N. Okong'o, J. Bellan, J. Comput. Phys. 176 (2002) 330.
[23] S.C.R. Dennis, G.-Z. Chang, J. Fluid Mech. 42 (1970) 471.
[24] B. Fornberg, J. Fluid Mech. 98 (1980) 819.
[25] M.N. Linnick, H.F. Fasel, J. Comput. Phys. 204 (2005) 157.